Energy Conversion and Management xxx (2009) xxx–xxx

Contents lists available at ScienceDirect

Energy Conversion and Management

journal homepage: www.elsevier.com/locate/enconman

A PSO based unified power flow controller for damping of power system oscillations

H. Shayeghi [a,*], H.A. Shayanfar [b], S. Jalilzadeh [c], A. Safari [c]

[a] Technical Engineering Department, University of Mohaghegh Ardabili, Daneshgah Street, P.O. Box 179, Ardabil, Iran
[b] Center of Excellence for Power Automation and Operation, Electrical Engineering Department, Iran University of Science and Technology, Tehran, Iran
[c] Technical Engineering Department, Zanjan University, Zanjan, Iran

ARTICLE INFO

Article history:
Received 27 September 2008
Received in revised form 26 May 2009
Accepted 8 June 2009
Available online xxxx

Keywords:
UPFC
PSO
Power system stability and control
Multiobjective optimization

ABSTRACT

On the basis of the linearized Phillips–Herffron model of a single-machine power system, we approach the problem of select the best input control signal of the unified power flow controller (UPFC) and design optimal UPFC based damping controller in order to enhance the damping of the power system low frequency oscillations. The potential of the UPFC supplementary controllers to enhance the dynamic stability is evaluated. This controller is tuned to simultaneously shift the undamped electromechanical modes to a prescribed zone in the s-plane. The problem of robustly UPFC based damping controller is formulated as an optimization problem according to the eigenvalue-based multiobjective function comprising the damping factor, and the damping ratio of the undamped electromechanical modes to be solved using particle swarm optimization technique (PSO) that has a strong ability to find the most optimistic results. To ensure the robustness of the proposed damping controller, the design process takes into account a wide range of operating conditions and system configurations. The effectiveness of the proposed controller is demonstrated through eigenvalue analysis, nonlinear time-domain simulation and some performance indices studies. The results analysis reveals that the tuned PSO based UPFC controller using the proposed multiobjective function has an excellent capability in damping power system low frequency oscillations and enhance greatly the dynamic stability of the power systems. Moreover, the system performance analysis under different operating conditions show that the δ_E based controller is superior to the m_B based controller.

1. Introduction

As power demand grows rapidly and expansion in transmission and generation is restricted with the limited availability of resources and the strict environmental constraints, power systems are today much more loaded than before. This causes the power systems to be operated near their stability limits. In addition, interconnection between remotely located power systems gives rise to low frequency oscillations in the range of 0.2–3.0 Hz. If not well damped, these oscillations may keep growing in magnitude until loss of synchronism results [1,2]. In order to damp these power system oscillations and increase system oscillations stability, the installation of power system stabilizer is both economical and effective. PSSs have been used for many years to add damping to electromechanical oscillations. However, PSSs suffer a drawback of being liable to cause great variations in the voltage profile and they may even result in leading power factor operation and losing system stability under severe disturbances, especially those three-phase faults which may occur at the generator terminals [3].

In recent years, the fast progress in the field of power electronics had opened new opportunities for the application of the FACTS devices as one of the most effective ways to improve power system operation controllability and power transfer limits [1–4]. Through the modulation of bus voltage, phase shift between buses, and transmission line reactance, FACTS devices can cause a substantial increase in power transfer limits during steady-state. Because of the extremely fast control action associated with FACTS-device operations, they have been very promising candidates for utilization in power system damping enhancement. It has been observed that utilizing a feedback supplementary control, in addition to the FACTS-device primary control, can considerably improve system damping and can also improve system voltage profile, which is advantageous over PSSs.

The unified power flow controller is regarded as one of the most versatile devices in the FACTS device family [5,6] which has the ability to control of the power flow in the transmission line, improve the transient stability, mitigate system oscillation and provide voltage support. It performs this through the control of the in-phase voltage, quadrate voltage and shunts compensation due to its mains control strategy [1,4]. The application of the UPFC to the modern power system can therefore lead to the more flexible, secure and economic operation [7]. When the UPFC is applied to

* Corresponding author. Tel.: +98 451 5517374; fax: +98 451 5512904.
E-mail address: hshayeghi@gmail.com (H. Shayeghi).

0196-8904/$ - see front matter © 2009 Elsevier Ltd. All rights reserved.
doi:10.1016/j.enconman.2009.06.009

Nomenclature

BT	boosting transformer
D	machine damping coefficient
DC	direct current
E'_q	internal voltage behind transient reactance
E_{fd}	equivalent excitation voltage
ET	excitation transformer
FACTS	flexible alternating current transmission systems
FD	figure of demerit
GA	genetic algorithm
GTO	gate turn off thyristor
ITAE	integral of the time multiplied absolute value of the error
K	proportional gain of the controller
K_A	regulator gain
M	machine inertia coefficient
m_E	excitation amplitude modulation ratio
m_B	boosting amplitude modulation ratio
OS	overshoot of speed deviation
P_e	active power
PI	proportional integral
P_m	mechanical input power
PSO	particle swarm optimization
PSS	power system stabilizer
SMIB	single machine infinite bus
SVC	static var compensator
T_1	lead time constant of controller
T_2	lag time constant of controller
T_3	lead time constant of controller
T_4	lag time constant of controller
T_A	regulator time constant
TCPS	thyristor controlled phase shifter
TCSC	thyristor controlled series compensator
T'_{do}	time constant of excitation circuit
T_e	electric torque
T_s	settling time of speed deviation
T_w	washout time constant
UPFC	unified power flow controller
US	undershoot of speed deviation
V	terminal voltage
v_{ref}	reference voltage
VSC	voltage source converter
ω	rotor speed
δ	rotor angle
δ_B	boosting phase angle
δ_E	excitation phase angle
ΔP_e	electrical power deviation
ΔV_{dc}	DC voltage deviation

the interconnected power systems, it can also provide significant damping effect on tie line power oscillation through its supplementary control.

Several trials have been reported in the literature to dynamic models of UPFC in order to design suitable controllers for power flow, voltage and damping controls [8]. Nabavi-Niaki and Iravani [9] developed a steady-state model, a small-signal linearized dynamic model, and a state-space large-signal model of a UPFC. So far, no work has been reported regarding the design of UPFC power oscillation damping controller with consideration of its closed-loop stability, dynamic tracking optimality and robustness against to variation of the power system operating conditions. Wang [10–12] presents the establishment of the linearized Phillips–Heffron model of a power system installed with a UPFC. He has not been presented a systematic approach for designing the damping controllers. Further, no effort seems to have been made to identify the most suitable UPFC control parameter, in order to arrive at a robust damping controller. Rouco [13] developed a novel unified Phillips–Heffron model for a power system equipped with a SVC, a TCSC and a TCPS. Damping torque coefficient analysis has been performed based on the proposed model to study the effect of FACTS controllers damping for different loading conditions. This model is the popular tools amongst power engineers for studying the dynamic behavior of synchronous generators, with a view to design control equipment. However, it only takes into account the generator main field winding and hence this model may not always yield a realistic dynamic assessment of the SMIB power system with FACTS, because the generator damping winding in q-axis is not considered in the system modeling. Huang et al. [14] attempted to design a conventional fixed-parameter lead-lag controller for a UPFC installed in the tie line of a two-area system to damp the inter-area mode of oscillations. A power frequency model for the UPFC has been derived with its DC link capacitor dynamics included to study the effects of the UPFC on power system stability. Moreover, a novel UPFC-network interface has been suggested in order to consideration of the UPFC model into the conventional transient stability analysis program with good convergence and accuracy in time simulation.

An industrial process, such as a power system, contains different kinds of uncertainties due to continuous load changes or parameters drift due to power systems highly nonlinear and stochastic operating nature. Consequently, a fixed parameter controller based on the classical control theory is not certainly suitable for the UPFC damping control design. Thus, it is required that a flexible controller be developed. Some authors suggested neural networks method [15] and robust control methodologies [7,16] to cope with system uncertainties to enhance the system damping performance using the UPFC. However, the parameters adjustments of these controllers need some trial and error. Also, although using the robust control methods, the uncertainties are directly introduced to the synthesis, but due to the large model order of power systems the order resulting controller will be very large in general, which is not feasible because of the computational economical difficulties in implementing. Also, some authors used fuzzy logic based damping control strategy for TCSC, UPFC and SVC in a multi-machine power system [17–19]. The damping control strategy employs non-optimal fuzzy logic controllers that is why the system's response settling time is unbearable. Moreover, the initial parameters adjustment of this type of controller needs some trial and error. Khon and Lo [20] used a fuzzy damping controller designed by micro-GA for TCSC and UPFC to improve the powers system low frequency oscillations. The proposed method may have not enough robustness due to its simplicity against the different kinds of uncertainties and disturbances. Mok et al. [21] applied a GA-based PI type fuzzy controller for UPFC to enhance power system damping. Although, the fuzzy PI controller is simpler and more applicable to remove the steady state error, it is known to give poor performance in the system transient response.

In this paper, PSO technique is used for the optimal tuning of UPFC based damping controller in order to enhance the damping of power systems low frequency oscillations and achieves the desired level of robust performance under different operating conditions and disturbances. PSO is a novel population based

Please cite this article in press as: Shayeghi H et al. A PSO based unified power flow controller for damping of power system oscillations. Energy Convers Manage (2009), doi:10.1016/j.enconman.2009.06.009

metaheuristic, which utilize the swarm intelligence generated by the cooperation and competition between the particle in a swarm and has emerged as a useful tool for engineering optimization. Unlike the other heuristic techniques, it has a flexible and well-balanced mechanism to enhance the global and local exploration abilities. Also, it suffices to specify the objective function and to place finite bounds on the optimized parameters. This algorithm has also been found to be robust in solving problems featuring non-linearity, non-differentiability and high-dimensionality [22–24].

In this study, the problem of robust UPFC based damping controller design is formulated as a multiobjective optimization problem. The multiobjective problem is concocted to optimize a composite set of two eigenvalue-based objective functions comprising the desired damping factor, and the desired damping ratio of the lightly damped and undamped electromechanical modes. The controller is automatically tuned with optimization an eigenvalue based multi-objective function by PSO to simultaneously shift the lightly damped and undamped electro-mechanical modes to a prescribed zone in the s-plane such that the relative stability is guaranteed and the time domain specifications concurrently secured. The effectiveness of the proposed controller is demonstrated through eigenvalue analysis, nonlinear time simulation studies and some performance indices to damp low frequency oscillations under different operating conditions. Results evaluation show that the proposed multiobjective function based tuned damping controller achieves good robust performance for a wide range of operating conditions and is superior to both designed controller using the single objective functions.

2. PSO technique

Particle swarm optimization algorithm, which is tailored for optimizing difficult numerical functions and based on metaphor of human social interaction, is capable of mimicking the ability of human societies to process knowledge [23]. It has roots in two main component methodologies: artificial life (such as bird flocking, fish schooling and swarming); and, evolutionary computation. Its key concept is that potential solutions are flown through hyperspace and are accelerated towards better or more optimum solutions. Its paradigm can be implemented in simple form of computer codes and is computationally inexpensive in terms of both memory requirements and speed. It lies somewhere in between evolutionary programming and the genetic algorithms. As in evolutionary computation paradigms, the concept of fitness is employed and candidate solutions to the problem are termed particles or sometimes individuals, each of which adjusts its flying based on the flying experiences of both itself and its companion. It keeps track of its coordinates in hyperspace which are associated with its previous best fitness solution, and also of its counterpart corresponding to the overall best value acquired thus far by any other particle in the population. Vectors are taken as presentation of particles since most optimization problems are convenient for such variable presentations. In fact, the fundamental principles of swarm intelligence are adaptability, diverse response, proximity, quality, and stability. It is adaptive corresponding to the change of the best group value. The allocation of responses between the individual and group values ensures a diversity of response. The higher dimensional space calculations of the PSO concept are performed over a series of time steps. The population is responding to the quality factors of the previous best individual values and the previous best group values. The principle of stability is adhered to since the population changes its state if and only if the best group value changes. As it is reported in [24], this optimization technique can be used to solve many of the same kinds of problems as GA, and does not suffer from some of GAs difficulties. It has also been found to be robust in solving problem featuring non-linearity, non-differentiability and high-dimensionality. PSO is the search method to improve the speed of convergence and find the global optimum value of fitness function.

PSO starts with a population of random solutions "particles" in a D-dimension space. The ith particle is represented by $X_i = (x_{i1}, x_{i2}, \ldots, x_{iD})$. Each particle keeps track of its coordinates in hyperspace, which are associated with the fittest solution it has achieved so far. The value of the fitness for particle i (pbest) is also stored as $P_i = (p_{i1}, p_{i2}, \ldots, p_{iD})$. The global version of the PSO keeps track of the overall best value (gbest), and its location, obtained thus far by any particle in the population. PSO consists of, at each step, changing the velocity of each particle toward its pbest and gbest according to Eq. (1). The velocity of particle i is represented as $V_i = (v_{i1}, v_{i2}, \ldots, v_{iD})$. Acceleration is weighted by a random term, with separate random numbers being generated for acceleration toward pbest and gbest. The position of the ith particle is then updated according to Eq. (2) [23].

$$v_{id} = w \times v_{id} + c_1 \times rand() \times (P_{id} - x_{id}) + c_2 \times rand() \times (P_{gd} - x_{id}) \tag{1}$$

$$x_{id} = x_{id} + c\,v_{id} \tag{2}$$

where P_{id} and P_{gd} are pbest and gbest. Several modifications have been proposed in the literature to improve the PSO algorithm speed and convergence toward the global minimum. One modification is to introduce a local-oriented paradigm (lbest) with different neighborhoods. It is concluded that gbest version performs best in terms of median number of iterations to converge. However, pbest version with neighborhoods of two is most resistant to local minima. PSO algorithm is further improved via using a time decreasing inertia weight, which leads to a reduction in the number of iterations [24]. Fig. 1 shows the flowchart of the proposed PSO algorithm.

This new approach features many advantages; it is simple, fast and easy to be coded. Also, its memory storage requirement is minimal. Moreover, this approach is advantageous over evolutionary and genetic algorithms in many ways. First, PSO has memory. That is, every particle remembers its best solution (local best) as well as the group best solution (global best). Another advantage of PSO is that the initial population of the PSO is maintained, and so there is no need for applying operators to the population, a process that is time and memory-storage-consuming. In addition, PSO is based on "constructive cooperation" between particles, in contrast with the genetic algorithms, which are based on "the survival of the fittest".

3. Description of case study system

Fig. 2 shows a SMIB power system equipped with a UPFC. The synchronous generator is delivering power to the infinite-bus through a double circuit transmission line and a UPFC. The UPFC consists of an excitation transformer, a boosting transformer, 2 three-phase GTO based voltage source converters, and a DC link capacitors. The four input control signals to the UPFC are m_E, m_B, δ_E, and δ_B.

3.1. Power system nonlinear model with UPFC

The dynamic model of the UPFC is required in order to study the effect of the UPFC for enhancing the small signal stability of the power system. The system data is given in the Appendix. By applying Park's transformation and neglecting the resistance and transients of the ET and BT transformers, the UPFC can be modeled as [10–12]:

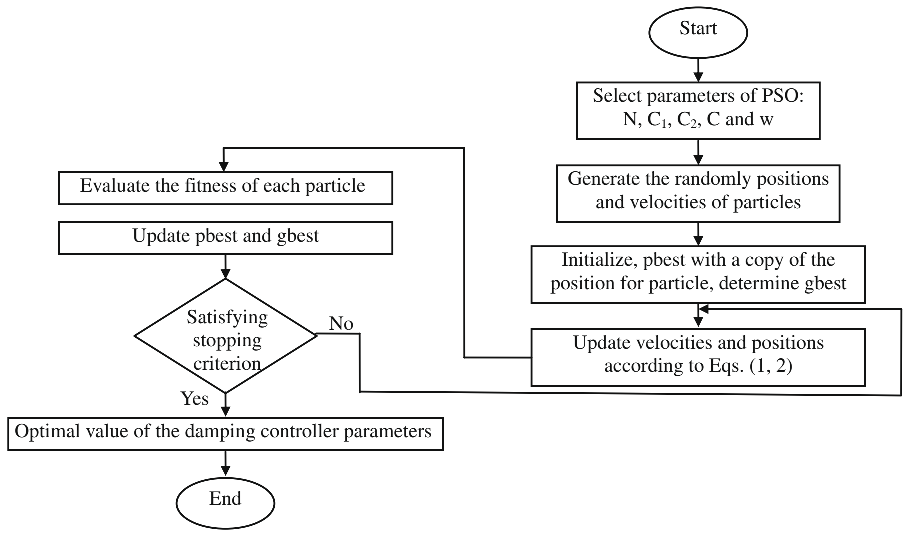

Fig. 1. Flowchart of the proposed PSO technique.

$$\begin{bmatrix} v_{Etd} \\ v_{Etq} \end{bmatrix} = \begin{bmatrix} 0 & -x_E \\ x_E & 0 \end{bmatrix} \begin{bmatrix} i_{Ed} \\ i_{Eq} \end{bmatrix} + \begin{bmatrix} \frac{m_E \cos\delta_E v_{dc}}{2} \\ \frac{m_E \sin\delta_E v_{dc}}{2} \end{bmatrix} \tag{3}$$

$$\begin{bmatrix} v_{Btd} \\ v_{Btq} \end{bmatrix} = \begin{bmatrix} 0 & -x_B \\ x_B & 0 \end{bmatrix} \begin{bmatrix} i_{Bd} \\ i_{Bq} \end{bmatrix} + \begin{bmatrix} \frac{m_B \cos\delta_B v_{dc}}{2} \\ \frac{m_B \sin\delta_B v_{dc}}{2} \end{bmatrix} \tag{4}$$

$$\dot{v}_{dc} = \frac{3m_E}{4C_{dc}} [\cos\delta_E \quad \sin\delta_E] \begin{bmatrix} i_{Ed} \\ i_{Eq} \end{bmatrix} + \frac{3m_B}{4C_{dc}} [\cos\delta_B \quad \sin\delta_B] \begin{bmatrix} i_{Bd} \\ i_{Bq} \end{bmatrix} \tag{5}$$

where v_{Et}, i_E, v_{Bt}, and i_B are the excitation voltage, excitation current, boosting voltage, and boosting current, respectively; C_{dc} and v_{dc} are the DC link capacitance and voltage. The nonlinear model of the SMIB system as shown in Fig. 2 is described by [1]

$$\dot{\delta} = \omega_0(\omega - 1) \tag{6}$$

$$\dot{\omega} = (P_m - P_e - D\Delta\omega)/M \tag{7}$$

$$\dot{E}'_q = (-E_q + E_{fd})/T'_{do} \tag{8}$$

$$\dot{E}_{fd} = (-E_{fd} + K_a(V_{ref} - V_t))/T_a \tag{9}$$

where

$$P_e = V_{td}I_{td} + V_{tq}I_{tq}; \quad E_q = E'_{qe} + (X_d - X'_d)I_{td};$$
$$V_t = V_{td} + jV_{tq}; \quad V_{td} = X_q I_{tq}; \quad V_{tq} = E'_q - X'_d I_{td};$$
$$I_{td} = I_{tld} + I_{Ed} + I_{Bd}; \quad I_{tq} = I_{tlq} + I_{Eq} + I_{Bq}$$

From Fig. 2 we can have:

$$\bar{v}_t = jx_{tE}(\bar{i}_B + \bar{i}_E) + \bar{v}_{Et} \tag{10}$$

$$\bar{v}_{Et} = \bar{v}_{Bt} + jx_{BV}\bar{i}_B + \bar{v}_b \tag{11}$$

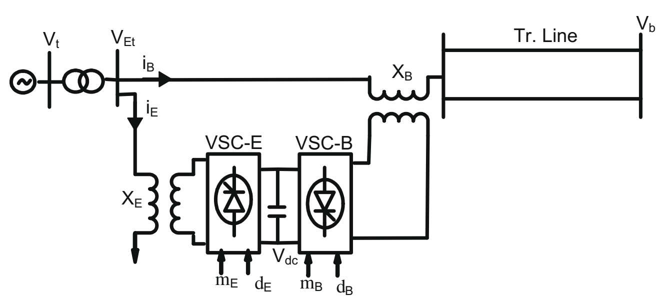

Fig. 2. SMIB power system equipped with UPFC.

$$v_{td} + jv_{tq} = x_q(i_{Eq} + i_{Bq}) + j(E'_q - x'_d(i_{Ed} + i_{Bd}))$$
$$= jx_{tE}(i_{Ed} + i_{Bd} + j(i_{Eq} + i_{Bq})) + v_{Etd} + jv_{Etq} \tag{12}$$

where i_t and v_b, are the armature current and infinite bus voltage, respectively. From the above equations, we can obtain:

$$i_{Ed} = \frac{x_{BB}}{x_{d\sum}} E'_q - \frac{m_E \sin\delta_E v_{dc} x_{Bd}}{2x_{d\sum}} + \frac{x_{dE}}{x_{d\sum}} \left(v_b \cos\delta + \frac{m_B \sin\delta_B v_{dc}}{2} \right) \tag{13}$$

$$i_{Eq} = \frac{m_E \cos\delta_E v_{dc} x_{Bq}}{2x_{q\sum}} - \frac{x_{qE}}{x_{q\sum}} \left(v_b \sin\delta + \frac{m_B \cos\delta_B v_{dc}}{2} \right) \tag{14}$$

$$i_{Bd} = \frac{x_E}{x_{d\sum}} E'_q + \frac{m_E \sin\delta_E v_{dc} x_{dE}}{2x_{d\sum}} - \frac{x_{dt}}{x_{d\sum}} \left(v_b \cos\delta + \frac{m_B \sin\delta_B v_{dc}}{2} \right) \tag{15}$$

$$i_{Bq} = -\frac{m_E \cos\delta_E v_{dc} x_{qE}}{2x_{q\sum}} + \frac{x_{qt}}{x_{q\sum}} \left(v_b \sin\delta + \frac{m_B \cos\delta_B v_{dc}}{2} \right) \tag{16}$$

where

$$x_{q\sum} = (x_q + x_T + x_E)\left(x_B + \frac{x_L}{2}\right) + x_E(x_q + x_T)$$
$$x_{Bq} = x_q + x_T + x_B + \frac{x_L}{2}$$
$$x_{qt} = x_q + x_T + x_E; \quad x_{qE} = x_q + x_T$$
$$x_{d\sum} = (x'_d + x_T + x_E)\left(x_B + \frac{x_L}{2}\right) + x_E(x'_d + x_T)$$
$$x_{Bd} = x'_d + x_T + x_B + \frac{x_L}{2}; \quad x_{Bd} = x'_d + x_T + x_E$$
$$x_{dE} = x'_d + x_T; \quad x_{BB} = x_B + \frac{x_L}{2}$$

x_E, x_B, x_d, x'_d and x_q are the ET, BT reactance's, d-axis reactance, d-axis transient reactance, and q-axis reactance, respectively.

3.2. Power system linearized model

A linear dynamic model is obtained by linearizing the nonlinear model round an operating condition. The linearized model of power system as shown in Fig. 2 is given as follows:

$$\Delta\dot{\delta} = \omega_0 \Delta\omega \tag{17}$$

$$\Delta\dot{\omega} = (-\Delta P_e - D\Delta\omega)/M \tag{18}$$

$$\Delta\dot{E}'_q = (-\Delta E_q + \Delta E_{fd})/T'_{do} \tag{19}$$

Please cite this article in press as: Shayeghi H et al. A PSO based unified power flow controller for damping of power system oscillations. Energy Convers Manage (2009), doi:10.1016/j.enconman.2009.06.009

$$\Delta \dot{E}_{fd} = (K_A(\Delta v_{ref} - \Delta v) - \Delta E_{fd})/T_A \tag{20}$$

$$\Delta \dot{v}_{dc} = K_7\Delta\delta + K_8\Delta E'_q - K_9\Delta v_{dc} + K_{ce}\Delta m_E + K_{c\delta e}\Delta\delta_E + K_{cb}\Delta m_B + K_{c\delta b}\Delta\delta_B \tag{21}$$

$$\Delta P_e = K_1\Delta\delta + K_2\Delta E'_q + K_{pd}\Delta v_{dc} + K_{pe}\Delta m_E + K_{p\delta e}\Delta\delta_E + K_{pb}\Delta m_B + K_{p\delta b}\Delta\delta_B \tag{22}$$

$$\Delta E'_q = K_4\Delta\delta + K_3\Delta E'_q + K_{qd}\Delta v_{dc} + K_{qe}\Delta m_E + K_{q\delta e}\Delta\delta_E + K_{qb}\Delta m_B + K_{q\delta b}\Delta\delta_B \tag{23}$$

$$\Delta V_t = K_5\Delta\delta + K_6\Delta E'_q + K_{vd}\Delta v_{dc} + K_{ve}\Delta m_E + K_{v\delta e}\Delta\delta_E + K_{vb}\Delta m_B + K_{v\delta b}\Delta\delta_B \tag{24}$$

$K_1, K_2, \ldots, K_9, K_{pu}, K_{qu}$ and K_{vu} are linearization constants. The state-space model of power system is given by:

$$\dot{x} = Ax + Bu \tag{25}$$

where the state vector x, control vector u, A and B are:

$$x = [\Delta\delta \quad \Delta\omega \quad \Delta E'_q \quad \Delta E_{fd} \quad \Delta v_{dc}]; \quad u = [\Delta m_E \quad \Delta\delta_E \quad \Delta m_B \quad \Delta\delta_B]^T$$

$$A = \begin{bmatrix} 0 & w_0 & 0 & 0 & 0 \\ -\frac{K_1}{M} & 0 & -\frac{K_2}{M} & 0 & -\frac{K_{pd}}{M} \\ -\frac{K_4}{T'_{do}} & 0 & -\frac{K_3}{T'_{do}} & \frac{1}{T'_{do}} & -\frac{K_{qd}}{T'_{do}} \\ -\frac{K_A K_5}{T_A} & 0 & -\frac{K_A K_6}{T_A} & -\frac{1}{T_A} & -\frac{K_A K_{vd}}{T_A} \\ K_7 & 0 & K_8 & 0 & -K_9 \end{bmatrix}$$

$$B = \begin{bmatrix} 0 & 0 & 0 & 0 \\ -\frac{K_{pe}}{M} & -\frac{K_{p\delta e}}{M} & -\frac{K_{pb}}{M} & -\frac{K_{p\delta b}}{M} \\ -\frac{K_{qe}}{T'_{do}} & -\frac{K_{q\delta e}}{T'_{do}} & -\frac{K_{qb}}{T'_{do}} & -\frac{K_{q\delta b}}{T'_{do}} \\ -\frac{K_A K_{vc}}{T_A} & -\frac{K_A K_{v\delta e}}{T_A} & -\frac{K_A K_{vb}}{T_A} & -\frac{K_A K_{v\delta b}}{T_A} \\ K_{ce} & K_{c\delta e} & K_{cb} & K_{c\delta b} \end{bmatrix}$$

The block diagram of the linearized dynamic model of the SMIB power system with UPFC is shown in Fig. 3.

3.3. UPFC based damping controller

The damping controller is designed to produce an electrical torque in phase with the speed deviation according to phase compensation method. The four control parameters of the UPFC (m_B, m_E, δ_B and δ_E) can be modulated in order to produce the damping torque.

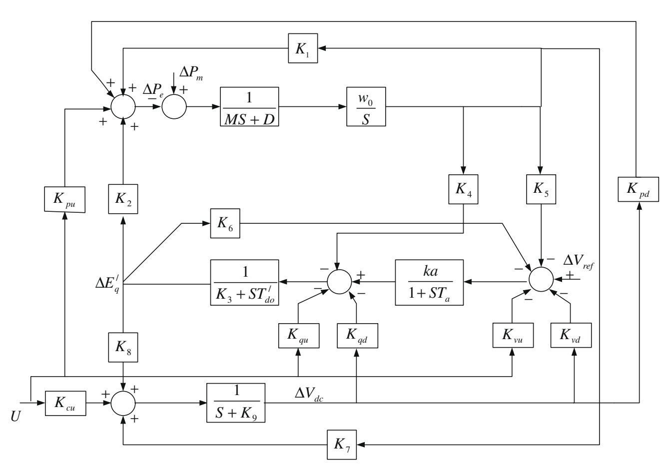

Fig. 3. Modified Heffron–Phillips transfer function model.

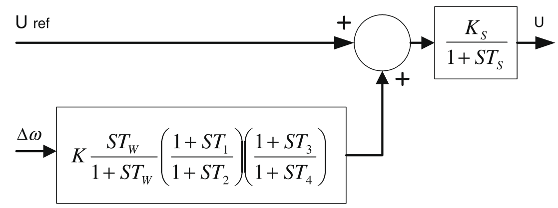

Fig. 4. UPFC with lead-lag controller.

In this paper δ_E and m_B are modulated in order to damping controller design. The speed deviation $\Delta\omega$ is considered as the input to the damping controller. The structure of UPFC based damping controller is shown in Fig. 4. This controller may be considered as a lead-lag compensator [1]. However, an electrical torque in phase with the speed deviation is to be produced in order to improve damping of the system oscillations. It comprises gain block, signal-washout block and lead-lag compensator. The parameters of the damping controller are obtained using PSO algorithm.

3.4. UPFC controller design using PSO

In the proposed method, we must tune the UPFC controller parameters optimally to improve overall system dynamic stability in a robust way under different operating conditions and disturbances. To acquire an optimal combination, this paper employs PSO [22] to improve optimization synthesis and find the global optimum value of fitness function. In this study, the PSO module works offline. For our optimization problem, an eigenvalue based multi objective function reflecting the combination of damping factor and damping ratio is considered as follows [25]:

$$J_3 = J_1 + aJ_2 \tag{26}$$

where $J_1 = \sum_{j=1}^{NP}\sum_{\sigma_i \geqslant \sigma_0}(\sigma_0 - \sigma_{i,j})^2$, $J_2 = \sum_{j=1}^{NP}\sum_{\zeta_i \leqslant \zeta_0}(\zeta_0 - \zeta_{i,j})^2$, $\sigma_{i,j}$ and $\zeta_{i,j}$ are the real part and the damping ratio of the ith eigenvalue of the jth operating point.

The value of α is chosen at 10. NP is the total number of operating points for which the optimization is carried out. The value of σ_0 determines the relative stability in terms of damping factor margin provided for constraining the placement of eigenvalues during the process of optimization. The closed loop eigenvalues are placed in the region to the left of dashed line as shown in Fig. 5a, if only J_1 were to be taken as the objective function. Similarly, if only J_2 is considered, then it limits the maximum overshoot of the eigenvalues as shown in Fig. 5b. In the case of J_2, ξ_0 is the desired minimum damping ratio which is to be achieved. When optimized with J_3, the eigenvalues are restricted within a D-shaped area as shown shaded in Fig. 5c.

It is necessary to mention here that only the unstable or lightly damped electromechanical modes of oscillations are relocated. The design problem can be formulated as the following constrained optimization problem, where the constraints are the controller parameters bounds:

$$\begin{aligned} &\text{Minimize} \quad J_i \\ &\text{Subject to} \quad K^{\min} \leqslant K \leqslant K^{\max} \\ &\qquad T_1^{\min} \leqslant T_1 \leqslant T_1^{\max} \\ &\qquad T_2^{\min} \leqslant T_2 \leqslant T_2^{\max} \\ &\qquad T_3^{\min} \leqslant T_3 \leqslant T_3^{\max} \\ &\qquad T_4^{\min} \leqslant T_4 \leqslant T_4^{\max} \end{aligned} \tag{27}$$

Typical ranges of the optimized parameters are [0.01–100] for K and [0.01–1] for T_1, T_2, T_3 and T_4. The proposed approach employs PSO algorithm to solve this optimization problem and search for an

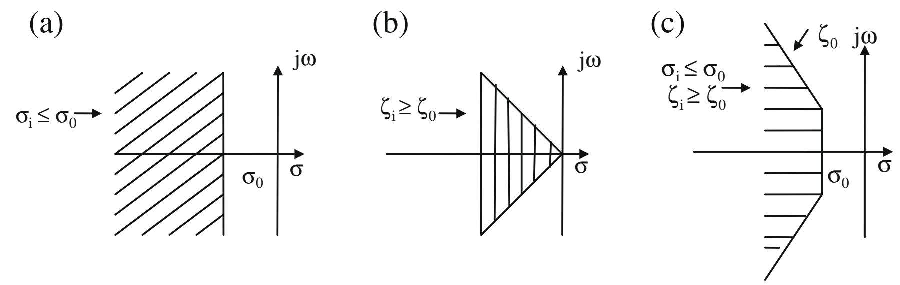

Fig. 5. Region of eigenvalue location for objective functions.

optimal or near optimal set of controller parameters. The optimization of UPFC controller parameters is carried out by evaluating the multiobjective cost function as given in Eq. (27), which considers a multiple of operating conditions. The operating conditions are considered as:

- Base case: $P = 0.80$ pu, $Q = 0.114$ pu and $X_L = 0.3$ pu.
- Case 1: $P = 0.2$ pu, $Q = 0.01$ and $X_L = 0.3$ pu.
- Case 2: $P = 1.20$ pu, $Q = 0.4$ and $X_L = 0.3$ pu.
- Case 3: $P = 0.80$ pu, $Q = 0.114$ pu and $X_L = 0.6$ pu.
- Case 4: $P = 1.20$ pu, $Q = 0.4$ and $X_L = 0.6$ pu.

In this study, the values of σ_0 and ζ_0 are taken as -2 and 0.3, respectively. In order to acquire better performance, number of particle, particle size, number of iteration, c_1, c_2, and c is chosen as 30, 5, 50, 2, 2 and 1, respectively. Also, the inertia weight, w, is linearly decreasing from 0.9 to 0.4. It should be noted that PSO algorithm is run several times and then optimal set of UPFC controller parameters is selected. The final values of the optimized parameters with both single objective functions J_1, J_2 and the multi-objective function J_3 are given in Table 1.

The electromechanical modes and the damping ratios obtained for all operating conditions both with and without proposed controllers in the system are given in Tables 2 and 3. When UPFC is not installed, it can be seen that some of the modes are poorly damped and in some cases, are unstable (highlighted in Tables 2 and 3). It is also clear that the system damping with the proposed J_3 based tuned UPFC controller are significantly improved. Moreover, it can be seen that electromechanical mode controllability via δ_E is higher than that m_B input.

4. Nonlinear time-domain simulation

To assess the effectiveness and robustness of the proposed controllers, simulation studies are carried out for various fault disturbances and fault clearing sequences for two scenarios.

4.1. Scenario 1

In this scenario, the performance of the proposed controller under transient conditions is verified by applying a 6-cycle three-phase fault at $t = 1$ s, at the middle of the one transmission line.

Table 1
The optimal parameter settings of the proposed controllers based on the different objective function based on the δ_E and m_B.

Controller parameters	δ_E			m_B		
	J_1	J_2	J_3	J_1	J_2	J_3
K	64.45	94.2	100	100	79.34	68.65
T_1	0.4185	0.2566	0.1069	0.6	0.3235	0.01
T_2	0.5299	0.1563	0.2022	0.3655	0.1424	0.1105
T_3	0.3835	0.1361	0.4347	0.5262	0.4523	0.4704
T_4	0.3507	0.0965	0.4134	0.4489	0.5094	0.1235

Table 2
Eigenvalues and damping ratios of electromechanical modes with and without δ_E controller.

Objective functions	Base case	Case 1	Case 2	Case 3	Case 4
Without controller	0.197 ± i4.51, −0.04 −2.99 ± i0.17, 0.99 −96.582	0.03 ± i5.32, −0.006 −2.7951, −3.1728 −96.268	0.285 ± i4.49, −0.06 −3.1878, −2.9126 −96.643	0.15 ± i4.03, −0.036 −3.18 ± i0.043, 0.99 −96.407	0.23 ± i3.88, −0.059 −3.3868, −3.0673 −96.48
J_1	−2.012 ± i6.994, 0.27 −2.772 ± i0.144, 0.98 −3.97, −1.8499 −96.544	−2.071 ± i6.984, 0.28 −2.788 ± i0.092, 0.99 −3.3636, −1.7719 −96.262	−2.112 ± i7.901, 0.25 −2.763 ± i0.125, 0.99 −4.3202, −1.8653 −96.598	−2.079 ± i7.256, 0.27 −2.894 ± i0.078, 0.99 −4.2825, −1.7806 −96.377	−2.160 ± i7.022, 0.29 2.887 ± i0.059, 0.99 −4.7938, −1.8063 −96.443
J_2	−1.031 ± i2.830, 0.34 −6.9885, −2.7324 −3.3804, −20.766 −96.403	−1.840 ± i2.946, 0.54 −2.7044, −3.2538 −22.579, −6.9473 −96.24	−0.9004 ± i2.801, 0.31 −7.016, −2.7103 −3.5115, −21.66 −96.427	−1.284 ± i2.075, 0.52 −24.963, −7.0502 −2.9761, −3.4973 −96.259	−1.130 ± i2.011, 0.49 −25.868, −7.0744 −3.6079, −2.965 −96.294
J_3	−2.961 ± i4.392, 0.56 −2.783 ± i2.264, 0.77 −2.460 ± i0.121, 0.99 −96.546	−3.173 ± i6.196, 0.45 −3.137 ± i0.736, 0.97 −2.428 ± i0.279, 0.98 −96.262	−3.337 ± i4.141, 0.63 −2.473 ± i2.638, 0.68 −2.468 ± i0.089, 0.99 −96.6	−4.206 ± i5.034, 0.64 −2.188 ± i1.333, 0.85 −2.5341, −2.7465 −96.378	−4.507 ± i4.918, 0.67 −2.949 ± i1.510, 0.89 −2.4526, −2.8285 −96.445

Please cite this article in press as: Shayeghi H et al. A PSO based unified power flow controller for damping of power system oscillations. Energy Convers Manage (2009), doi:10.1016/j.enconman.2009.06.009

Table 3
Eigenvalues and damping ratios of electromechanical modes with and without m_B controller.

Objective functions	Base case	Case 1	Case 2	Case 3	Case 4
Without controller	0.197 ± i4.51, −0.04 −2.99 ± i0.17, 0.99 −96.582	0.03 ± i5.32, −0.006 −2.7951, −3.1728 −96.268	0.285 ± i4.49, −0.06 −3.1878, −2.9126 −96.643	0.15 ± i4.03, −0.036 −3.18 ± i0.043,0.99 −96.407	0.23 ± i3.88, −0.059 −3.3868, −3.0673 −96.48
J_1	−2.075 ± i6.844, 0.28 −2.019 ± i1.779, 0.75 −2.227 ± i0.026, 0.999 −96.764	−2.197 ± i7.063, 0.289 −2.806 ± i1.318, 0.9 −2.5071, −2.1509 −96.351	−2.015 ± i7.801, 0.25 −2.969 ± i1.873, 0.84 −2.217 ± i0.069, 0.99 −96.842	−2.060 ± i6.744, 0.289 −2.749 ± i1.736, 0.84 −2.6419, −2.1348 −96.504	−2.067 ± i7.454, 0.267 −2.794 ± i1.951, 0.82 −2.6123, −2.1367 −96.587
J_2	−1.323 ± i4.027, 0.312 −3.121 ± i0.249, 0.997 −1.9436, −6.6017 −96.737	−1.103 ± i3.008, 0.34 −7.5057, −1.9445 −3.1945, −2.8223 −96.339	−1.406 ± i4.207, 0.32 −6.548, −1.947 −3.0151, −3.477 −96.812	−1.786 ± i3.847, 0.42 −7.173, −1.9377 −3.135, −3.3676 −96.489	−1.1739 ± i3.684, 0.304 −7.1849, −1.9378 −3.5778, −3.0725 −96.571
J_3	−2.668 ± i4.105, 0.545 −3.647 ± i3.652, 0.706 −2.6635, −7.8836 −96.581	−2.69 ± i5.159, 0.462 −6.791 ± i3.813, 0.87 −3.7891, −2.7154 −96.267	−3.928 ± i4.463, 0.66 −2.409 ± i3.613, 0.55 −2.643, −7.8342 −96.642	−2.098 ± i3.795, 0.48 −6.841 ± i3.024, 0.91 −4.7565, −2.8963 −96.406	−2.027 ± i3.595, 0.49 −6.725 ± i3.282, 0.89 −5.0951, −2.8801 −96.479

The fault is cleared by permanent tripping of the faulted line. The performance of the controllers when the multiobjective function is used in the design is compared to that of the controllers designed using the single objective functions J_1 and J_2. The speed deviation of generator at base case, case 2 and case 4 due to designed controller based on the δ_E and m_B are shown in Figs. 6 and 7. Also, Figs. 8 and 9 show the electrical power deviation, internal voltage variations and DC voltage deviation with δ_E and m_B controllers, respectively. It can be seen that the PSO based UPFC controller tuned using the multiobjective function achieves good robust performance, provides superior damping in comparison with the other objective functions and enhance greatly the dynamic stability of power systems.

4.2. Scenario 2

In this scenario, another severe disturbance is considered for different loading conditions; that is, a 6-cycle, three-phase fault is applied at the same above mentioned location in scenario 1. The fault is cleared without line tripping and the original system is restored upon the clearance of the fault. The system response to this disturbance is shown in Figs. 10 and 11. It can be seen that the proposed multiobjective function based optimized UPFC controller has good performance in damping low frequency oscillations and stabilizes the system quickly.

From the above conducted tests, it can be concluded that the δ_E based damping controller is superior to the m_B based damping controller.

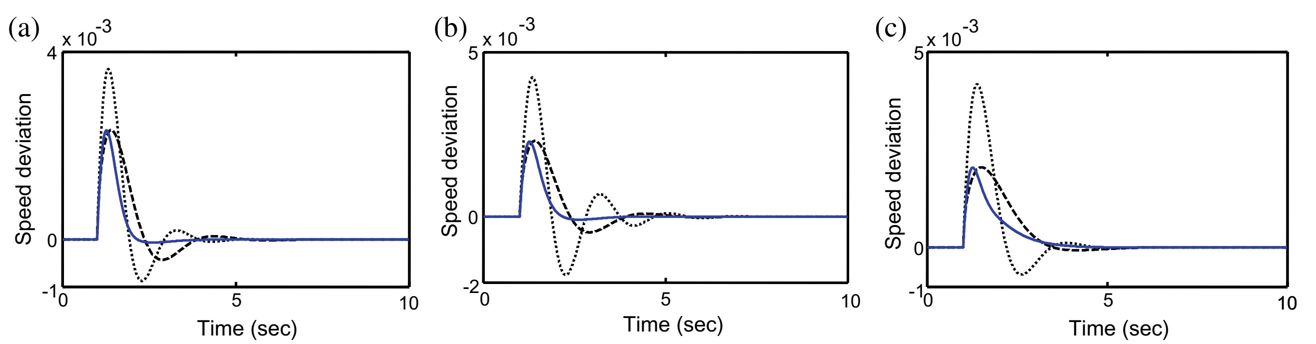

Fig. 6. Dynamic responses for $\Delta\omega$ in scenario 1 with δ_E controller at (a) Base case (b) Case 2 and (c) Case 4 loading conditions; solid (J_3), dashed (J_2) and dotted (J_1).

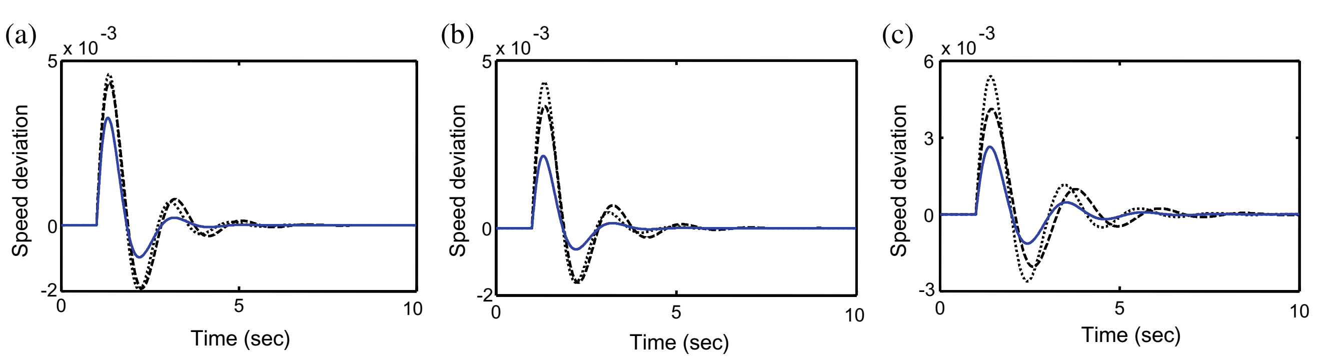

Fig. 7. Dynamic responses for $\Delta\omega$ in scenario 1 with m_B controller at (a) Base case (b) Case 2 and (c) Case 4 loading conditions; solid (J_3), dashed (J_2) and dotted (J_1).

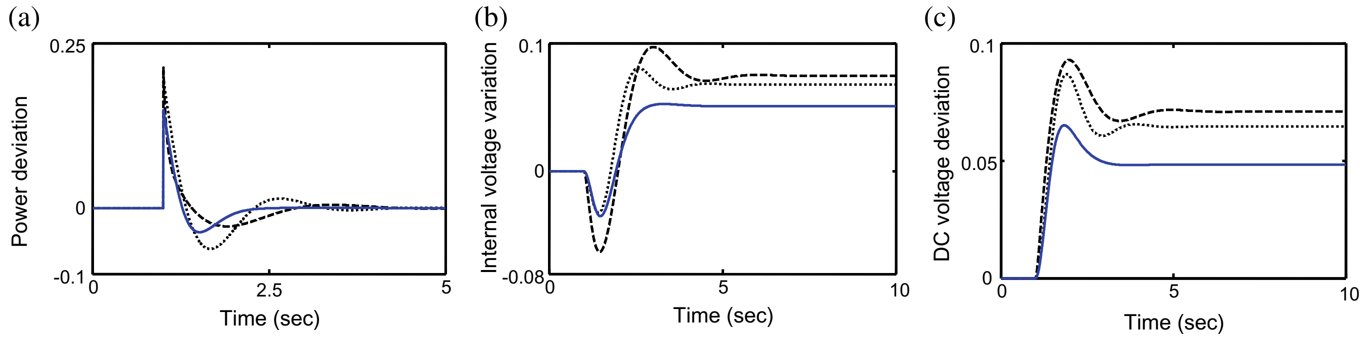

Fig. 8. Dynamic responses in scenario 1 with δ_E controller at base case loading (a) ΔP_e (b) ($\Delta E'_q$) and (c) ΔV_{dc}; solid (J_3), dashed (J_2) and dotted (J_1).

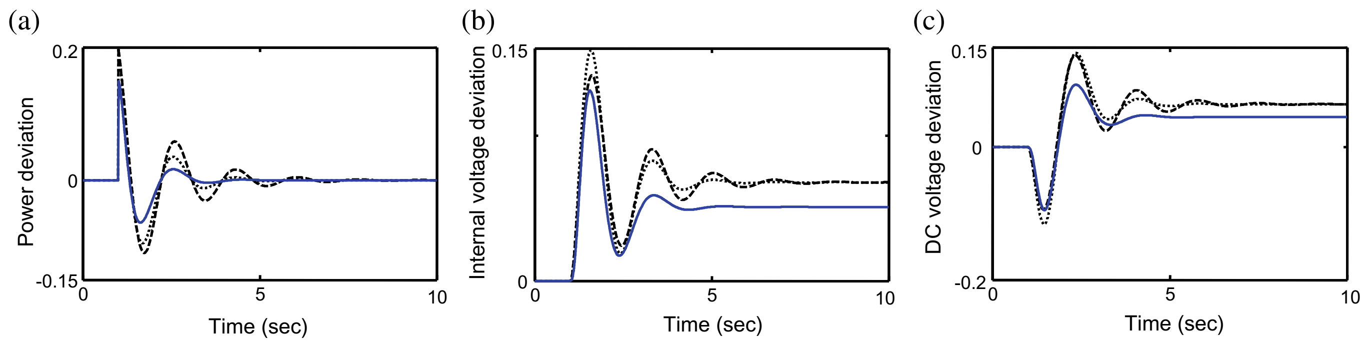

Fig. 9. Dynamic responses in scenario 1 with m_B controller at base case loading (a) ΔP_e (b) ($\Delta E'_q$) and (c) ΔV_{dc}; solid (J_3), dashed (J_2) and dotted (J_1).

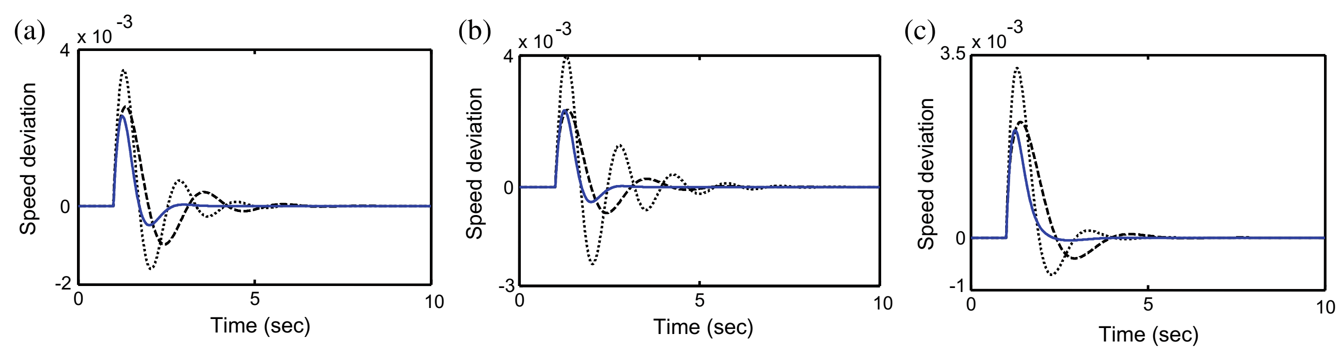

Fig. 10. Dynamic responses for $\Delta\omega$ in scenario 2 with δ_E controller at (a) Base case (b) Case 2 and (c) Case 4 loading conditions; solid (J_3), dashed (J_2) and dotted (J_1).

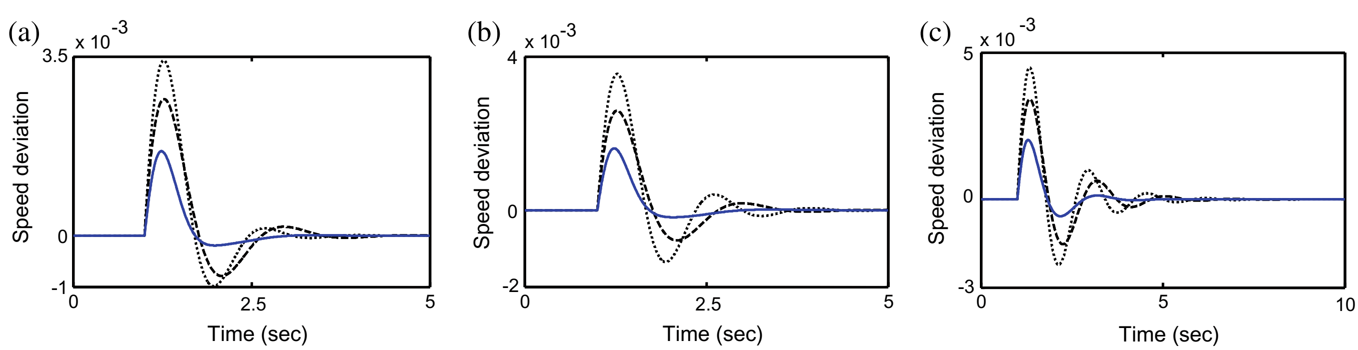

Fig. 11. Dynamic responses for $\Delta\omega$ in scenario 2 with m_B controller at (a) Base case (b) Case 2 and (c) Case 4 loading conditions; solid (J_3), dashed (J_2) and dotted (J_1).

To demonstrate performance robustness of the proposed method, two performance indices: the ITAE and FD based on the system performance characteristics are defined as [26]:

$$\begin{aligned} \mathrm{ITAE} &= 100\int_0^5 (|\Delta P_e| + |\Delta V_{dc}| + |\Delta\omega|)\cdot t dt \\ FD &= (\mathrm{OS}\times 1000)^2 + (\mathrm{US}\times 4000)^2 + T_s^2 \end{aligned} \tag{28}$$

Table 4
Values of performance index ITAE.

Fault case	Objective function	Base case		Case 1		Case 2		Case 3		Case 4	
		δ_E	m_B	δ_E	m_B	δ_E	m_B	δ_E	m_B	δ_E	m_B
With tripping line	J_1	2.525	3.045	2.181	2.744	2.314	2.867	2.06	4.014	1.939	4.066
	J_2	2.722	3.558	2.383	3.225	2.495	3.39	2.346	4.872	2.228	5.047
	J_3	1.726	2.153	1.595	1.894	1.56	2.033	1.569	2.773	1.484	2.789
Without tripping line	J_1	2.719	2.562	2.441	2.54	2.459	2.294	2.084	2.596	1.898	2.48
	J_2	2.850	2.798	2.612	2.837	2.573	2.52	2.272	3.038	2.066	2.961
	J_3	1.804	1.869	1.762	1.802	1.58	1.675	1.455	1.831	1.297	1.747

Table 5
Values of performance index FD.

Fault case	Objective function	Base case		Case 1		Case 2		Case 3		Case 4	
		δ_E	m_B	δ_E	m_B	δ_E	m_B	δ_E	m_B	δ_E	m_B
With tripping line	J_1	38.89	90.14	16.747	100.41	40.44	88.75	20.85	223.14	21.848	235.33
	J_2	21.586	148.42	12.73	147.4	22.63	149.14	16.07	338.64	15.86	365.72
	J_3	9.566	38.94	8.76	44.74	9.58	38.37	15.01	105.68	15.74	111.12
Without tripping line	J_1	64.75	28.76	24.675	46.37	74.453	27.86	28.05	77.38	31.45	79.08
	J_2	31.365	59.61	11.615	75.23	41.937	59.22	17.91	134.6	15.86	134.58
	J_3	14.72	14.31	7.74	16.77	15.42	14.17	8.416	33.1	15.74	34.16

Table 6
System parameters.

Generator		
$M = 8$ MJ/MVA	$T'_{do} = 5.044$ s	$X_d = 1$ pu
$X_q = 0.6$ pu	$X'_d = 0.3$ pu	$D = 0$
Excitation system	$K_a = 10$	$T_a = 0.05$ s
Transformers	$X_T = 0.1$ pu	$X_E = 0.1$ pu
	$X_B = 0.1$ pu	
Transmission line	$X_L = 1$ pu	
Operating condition	$P = 0.8$ pu	$V_b = 1.0$ pu
	$V_t = 1.0$ pu	
DC link parameter	$V_{DC} = 2$ pu	$C_{DC} = 1$ pu
UPFC parameter	$m_B = 0.08$	$\delta_B = -78.21°$
	$\delta_E = -85.35°$	$m_E = 0.4$
	$K_s = 1$	$T_s = 0.05$

where speed deviation, electrical power deviation, DC voltage deviation, Overshoot, Undershoot and settling time of speed deviation of the machine is considered for evaluation of the ITAE and FD indices. It is worth mentioning that the lower the value of these indices is, the better the system response in terms of time-domain characteristics. Numerical results of performance robustness for all system loading cases are listed in Tables 4 and 5. It can be seen that the values of these system performance characteristics with the J_3 based tuned controller are much smaller compared to J_1 and J_2 based tuned stabilizers. This demonstrates that the overshoot, undershoot, settling time and speed deviations of the machine are greatly reduced by applying the proposed J_3 based tuned controller. Moreover, it can be concluded that the δ_E controller is the most robust controller.

5. Conclusions

In this paper, transient stability performance improvement by a UPFC controller has been investigated. The stabilizers are tuned to simultaneously shift the undamped electromechanical modes of the machine to a prescribed zone in the s-plane. A multiobjective problem is formulated to optimize a composite set of objective functions comprising the damping factor, and the damping ratio of the undamped electromechanical modes. The design problem of the controller is converted into an optimization problem which is solved by a PSO technique with the eigenvalue-based multiobjective function. The effectiveness of the proposed UPFC controllers for improving transient stability performance of a power system are demonstrated by a weakly connected example power system subjected to different severe disturbances. The eigenvalue analysis and non-linear time domain simulation results show the effectiveness of the proposed controller using multiobjective function and their ability to provide good damping of low frequency oscillations. The system performance characteristics in terms of 'ITAE' and 'FD' indices reveal that the proposed multiobjective function based tuned stabilizers demonstrates its superiority than both the designed stabilizers using J_1 and J_2 at various fault disturbances and fault clearing sequences.

Appendix A

The nominal parameters and operating condition of the system are listed in Table 6.

References

[1] Al-Awami AT, Abdel-Magid YL, Abido MA. A particle-swarm-based approach of power system stability enhancement with unified power flow controller. Elect Power Energy Syst 2007;29:251–9.
[2] Anderson PM, Fouad AA. Power System Control and Stability. Ames (IA): Iowa State Univ. Press; 1977.
[3] Keri AJF, Lombard X, Edris AA. Unified power flow controller: modeling and analysis. IEEE Trans Power Deliv 1999;14(2):648–54.
[4] N. Tambey, M. Kothari, Unified power flow controller based damping controllers for damping low frequency oscillations in a power system; 2003. <http://www.ieindia.org/publish/el/0603>.
[5] Gyugyi L. Unified power-flow control concept for flexible ac transmission systems. IEE Proc Gen Transm Distrib 1992;139(4):323–31.
[6] Hingorani NG, Gyugyi L. Understanding FACTS: concepts and technology of flexible AC transmission systems. Wiley-IEEE Press; 1999.
[7] Vilathgamuwa M, Zhu X, Choi SS. A robust control method to improve the performance of a unified power flow controller. Elect Power Syst Res 2000;55: 103–11.
[8] Song YH, Johns AT. Flexible ac transmission systems (FACTS). UK: IEE Press; 1999.
[9] Nabavi-Niaki A, Iravani MR. Steady-state and dynamic models of unified power flow controller (UPFC) for power system studies. IEEE Trans Power Syst 1996;11(4):1937–43.
[10] Wang HF. A unified model for the analysis of FACTS devices in damping power system oscillations – Part III: unified power flow controller. IEEE Trans Power Deliv 2000;15(3):978–83.

[11] Wang HF. Damping function of unified power flow controller. IEE Proc Gen Transm Distrib 1999;146(1):81–7.
[12] Wang HF. Application of modeling UPFC into multi-machine power systems. IEE Proc Gen Transm Distrib 1999;146(3):306–12.
[13] Rouco L. Coordinated design of multiple controllers for damping power system oscillations. Elect Power Energy Syst 2001;23:517–30.
[14] Huang Z, Ni Y, Shen CM, Mu FF, Chen S, Zhang B. Application of unified power flow controller in interconnected power systems-modeling interface control strategy and case study. IEEE Trans Power Syst 2000;5(2):817–24.
[15] Dash PK, Mishra S, Panda G. A radial basis function neural network controller for UPFC. IEEE Trans Power Syst 2000;5(4):1293–9.
[16] Pal BC. Robust damping of interarea oscillations with unified power flow controller. IEE Proc Gen Transm Distrib 2002;149(6):733–8.
[17] Kazemi A, Vakili Sohrforouzani M. Power system damping controlled facts devices. Elect Power Energy Syst 2006;28:349–57.
[18] Dash PK, Mishra S, Panda G. Damping multimodal power system oscillation using hybrid fuzzy controller for series connected FACTS devices. IEEE Trans Power Syst 2000;15(4):1360–6.
[19] Limyingcharone S, Annakkage UD, Pahalawaththa NC. Fuzzy logic based unified power flow controllers for transient stability improvement. IEE Proc Gen Transm Distrib 1998;145(3):225–32.
[20] Khon L, Lo KL. Hybrid micro-GA based FLCs for TCSC and UPFC in a multi machine environment. Elect Power Syst Res 2006;76:832–43.
[21] Mok TK, Liu H, Ni Y, Wu FF, Hui R. Tuning the fuzzy damping controller for UPFC through genetic algorithm with comparison to the gradient descent training. Elect Power Energy Syst 2005;27:275–83.
[22] Shayeghi H, Jalili A, Shayanfar HA. Multi-stage fuzzy load frequency control using PSO. Energy Convers Manage 2008;49:2570–80.
[23] Kennedy J, Eberhart R, Shi Y. Swarm intelligence. San Francisco: Morgan Kaufmann Publishers; 2001.
[24] Clerc M, Kennedy J. The particle swarm-explosion, stability, and convergence in a multidimensional complex space. IEEE Trans Evolut Comput 2002;6(1): 58–73.
[25] Abdel-Magid YL, Abido MA. Optimal multiobjective design of robust power system stabilizers using genetic algorithms. IEEE Trans Power Syst 2003;18(3): 1125–32.
[26] Shayeghi H, Shayanfar HA, Jalili A. Multi stage fuzzy PID power system automatic generation controller in deregulated environments. Energy Convers Manage 2006;47:2829–45.

Please cite this article in press as: Shayeghi H et al. A PSO based unified power flow controller for damping of power system oscillations. Energy Convers Manage (2009), doi:10.1016/j.enconman.2009.06.009